

APPLIED RESEARCH

PI Observer for Actuator Fault Estimation in a Distillation Process: A Descriptor Approach

MARLEM FLORES-MONTIEL^{1,2}, (Member, IEEE), CARLOS MANUEL ASTORGA-ZARAGOZA¹,
GLORIA LILIA OSORIO-GORDILLO¹, RODOLFO AMALIO VARGAS-MÉNDEZ¹,
PORFIRIO-ROBERTO NÁJERA-MEDINA², AND ANGÉLICA GÓMEZ-CÁRDENAS²

¹CENIDET, Tecnológico Nacional de México, Cuernavaca 62490, Mexico

²Instituto Tecnológico de Cuautla, Tecnológico Nacional de México Campus, Yecapixtla 62826, Mexico

Corresponding author: Carlos Manuel Astorga-Zaragoza (carlos.az@cenidet.tecnm.mx)

ABSTRACT This paper presents a Proportional-Integral observer (PIO) that allows simultaneous states and unknown input estimation. The goal of this observer is to perform actuator fault estimation for a distillation process by using a simplified mathematical model. This model describes the intrinsic physical characteristics of the process through a descriptor Linear Parameter Varying (LPV) approach. The stability of the observer is analyzed through a Lyapunov stability theory. The proposed scheme estimates a fault in a peristaltic pump that feeds the distillation column. The main contribution is demonstrating the generalization of the descriptor LPV approach, expanding the potential applications of modern control strategies for fault estimation in nonlinear processes, especially in distillation plants.

INDEX TERMS Actuator fault estimation, distillation process, PI observer, descriptor LPV systems.

I. INTRODUCTION

Typically industrial plate distillation columns have large dynamic models due to the great number of stages (N-plates, a boiler, and a condenser). Even the simplest dynamic model of distillation columns is complex because the nonlinear differential equations must be at least equal to the number of column stages. However, this complexity can be reduced by considering a technique based on singular perturbation theory, presented in [1], which generates a reduced-order model by separating the fast and slow dynamics of the process. This technique allows to approximating the compartment dynamics by differential equations for a representative stage with a holdup equivalent to the total compartment holdup. In [2], this approach is applied to a high-purity air separation process.

Descriptor dynamical systems are often used as an alternative modeling approach to typical dynamical models described only with differential equations. The advantage of the descriptor approach is to represent a wider range of practical processes, such as electrical [4], [5], electronic [6], [7], chemical [8], [9], and mechatronic systems [10], [11].

The associate editor coordinating the review of this manuscript and approving it for publication was Giambattista Gruosso¹.

These systems can preserve the original system's physical structure while accounting for non-dynamic constraints and impulsive behavior. The algebraic equations act as constraints for the differential part of the system [3].

On the other hand, Linear Parameter Varying (LPV) systems are a class of nonlinear systems represented in a state-affine and control-affine form, but one or more parameters are time-variant. LPV systems theory may have many practical applications due to their special structure [12]. First, they can be treated as Linear Time-Invariant systems subject to a time-varying parameter vector $\rho(t) = [\rho_1(t) \ \rho_2(t), \dots, \rho_J(t)]$. Alternatively, LPV systems can also be linear time-varying models resulting from linearizing nonlinear plants along the parameter ρ trajectories. This transformation is achieved without any loss of information and produces a system with the same state trajectory as the original system [13], [14], [15], [16].

The task of estimating state variables, system parameters or unknown inputs is crucial in diagnostic systems. In order to detect changes in the correlation between state variables, researchers design model-based estimation algorithms [17], [18], [19]. In particular, the observer design for descriptor systems has received considerable attention because the effectivity of the methods. These methods have been

extended to nonlinear descriptor systems. For instance, some works about full and reduced-order observers can be found in [20], [21], [22]; a Proportional-Integral observer for systems with unknown inputs can be read in [23], [24], [25], whereas an Unknown Input Observer (UIO) for nonlinear descriptor systems is presented in [26]. A Luenberger observer with a parametric approach is used in [27], and an adaptive fuzzy observer for nonlinear descriptor systems is considered in [28].

Most existing Fault Detection and Diagnosis (FDD) methods rely on designing appropriate observers. Some researchers have proposed fault diagnosis systems for descriptor systems, such as the one presented in [29], where a UIO is used for detecting, isolating, and reconstructing actuator and sensor faults, but not all at once. In [30], a polytopic UIO is designed for descriptor LPV systems to estimate the system states in the presence of unknown inputs.

The first step in fault accommodation is to perform a Fault Detection and Isolation (FDI) process. This process monitors the system and identifies the location of the fault. In [31], an FDI scheme uses a linear sliding mode observer for actuator and sensor faults. This scheme is applied to a distillation column process. Online fault estimation is then used to determine the magnitude of the fault. This enables the implementation of an active Fault Tolerant Control (FTC) system through either fault accommodation or system reconfiguration [32].

The main contribution of this study involves developing a descriptor LPV model to implement a fault estimation technique utilizing a PI observer for the distillation process. The LPV descriptor model obtained is then compared in simulation with data from the nonlinear model of a five-tray distillation column using an ethanol-water mixture. The study combines local linear descriptor models, which are interpolated using appropriate weight functions, to determine the influence of each local model on the overall system behavior. Another contribution of this research is to demonstrate the simplification of a nonlinear system into a multi-linear system in polytopic form, using the model reduction technique proposed by [8] to establish a descriptor LPV model for distillation columns. This model could be used for developing accurate actuator fault estimation techniques. The efficacy of the approach is evaluated through numerical simulations.

This work distinguishes itself through several key advancements compared to prior research: (i) It extends the applicability of the methodology to a broader class of nonlinear processes affected by unknown inputs or disturbances, facilitating the estimation of both process variables and unknown inputs, (ii) by incorporating the descriptor LPV approach into the design, the PI observer demonstrates enhanced estimation performance, (iii) the simplicity of computing observer gains, through solving a simple set of LMIs, eliminating the necessity to solve additional differential equations typically associated with Kalman observers.

II. FAULT ESTIMATION BASED ON PROPORTIONAL INTEGRAL OBSERVER DESIGN

A. PROPORTIONAL INTEGRAL OBSERVER DESIGN

An approach to achieving a multi-model structure involves a collection of linear models scheduled by weighting functions to represent polytopic LPV models, as outlined in [33]. Utilizing this representation, some authors have developed fault diagnosis methods for nonlinear systems described by Takagi-Sugeno models, such as the one presented in [34]. Furthermore, techniques like those demonstrated in [19] utilize observer models for detecting and isolating actuator faults in differential-algebraic LPV systems represented by a polytopic form. Another interesting alternative is to consider adjustable dimension observers as presented in [35] where fault estimation is performed for switched fuzzy systems with unmeasurable premise variables, or reduced-order observers for finite-time fault estimation for switched systems and time varying faults [36]. In [37], fault reconstruction and fault-tolerant control of switched fuzzy systems with actuator and sensor faults are addressed. Although these three last approaches are effective methods for fault estimation, they are designed specifically for switched systems.

In this work descriptor systems having the following (non-switched) LPV form are considered:

$$\begin{aligned} E\dot{x}(t) &= \sum_{i=1}^{2^J} \varepsilon_i(\rho(t)) (A_i x(t) + B_i u(t) + R_i d(t)), \\ y(t) &= Cx(t), \end{aligned} \quad (1)$$

where $x(t) \in \mathbb{R}^m$ represents the semi-state vector, $u(t) \in \mathbb{R}^k$ is the input vector, $d \in \mathbb{R}^l$ is an unknown input, and $y \in \mathbb{R}^p$ is the output vector. $E \in \mathbb{R}^{m \times m}$ is a matrix with $\text{rank}(E) = r \leq m$. $A_i \in \mathbb{R}^{m \times m}$, $B_i \in \mathbb{R}^{m \times k}$, $R_i \in \mathbb{R}^{m \times l}$ and $C \in \mathbb{R}^{p \times m}$ are known constant matrices. $\rho(t) = [\rho_1, \dots, \rho_J]$ is the vector of J variant parameters. Furthermore, it is assumed that $\rho(t)$ is available (i.e., perfectly measurable) for the observer, which will be proposed.

In this paper, the polytopic case is treated, where a polytope is a geometric object in a hypercube with 2^J dimensions. It has several vertices, edges, and faces. In this scenario, the vertices of the polytope are obtained by combining different weighting functions. These functions assign a weight to each parameter or variable in a dataset, which creates a linear combination. This linear combination serves as the basis for the global model that can be used to analyze the dataset. Under this consideration the weighted functions $\varepsilon_i(\rho(t))$ have the following properties:

$$\sum_{i=1}^{2^J} \varepsilon_i(\rho(t)) = 1, \quad 0 \leq \varepsilon_i(\rho(t)) \leq 1. \quad (2)$$

Definition 1 [46]: Consider that system (1) has the following slow and fast subsystems

$$\dot{x}_a(t) = \sum_{i=1}^{2^J} \varepsilon_i(\rho(t)) (A_{ia} x_a(t) + B_{ia} u(t) + R_{ia} d(t)),$$

$$y_a(t) = C_a x_a(t), \quad (3)$$

and

$$N \dot{x}_b(t) = \sum_{i=1}^{2^J} \varepsilon_i(\rho(t)) (x_b(t) + B_{ib}u(t) + R_{ib}d(t)),$$

$$y_b(t) = C_b x_b(t), \quad (4)$$

where $x_a(t) \in \mathbb{R}^{m_a}$, $x_b(t) \in \mathbb{R}^{m_b}$, $m_a + m_b = m$, the matrix $N \in \mathbb{R}^{m_b \times m_b}$ is nilpotent.

- 1) The slow system (3) is observable if and only if, from system (1)

$$\text{rank} \begin{bmatrix} sE - A \\ C \end{bmatrix} = n, \quad \forall s \in \mathbb{C}, \quad s \text{ finite.} \quad (5)$$

- 2) The fast subsystem (4) is observable if and only if, from system (1)

$$\text{rank} \begin{bmatrix} E \\ C \end{bmatrix} = n. \quad (6)$$

- 3) System (3) is observable if and only if conditions (5)-(6) and (1) hold, or

$$\text{rank} \begin{bmatrix} \alpha E - \beta A \\ C \end{bmatrix} = n, \quad \forall (\alpha, \beta) \in \mathbb{C}^2 \setminus \{(0, 0)\}. \quad (7)$$

Assumption 1 The system (1) is called observable if conditions of Definition 1 are verified, which reflects the reconstruction ability of the whole state $x(t)$ from measured output together with the control input.

Assumption 2 The system (1) is regular; this property guarantees the existence and uniqueness of solutions if there exists a constant scalar $\gamma \in \mathbb{C}$ such that

$$\det(\gamma E - A_i) \neq 0, \quad (8)$$

or equivalently, the polynomial $\det(sE - A_i)$ is not identically zero.

Assumption 3 It is assumed that the $\text{rank}(CR_i) = \text{rank}(R_i)$. This Assumption implies that $p \geq l$, the number of measurable outputs must be greater than or equal to the number of faults [45].

Consider the following LPV PI Observer for system (1):

$$\dot{Z}(t) = \sum_{i=1}^{2^J} \varepsilon_i(\rho(t)) \left[N_i Z(t) + G_i u(t) + L_i y(t) + H_i \hat{d}(t) \right], \quad (9)$$

$$\dot{\hat{d}}(t) = \sum_{i=1}^{2^J} \varepsilon_i(\rho(t)) \Phi_i(y(t) - \hat{y}(t)), \quad (10)$$

$$\hat{x}(t) = Z(t) + M y(t). \quad (11)$$

In the PI observer there are three vectors: $Z(t) \in \mathbb{R}^m$, $\hat{d}(t) \in \mathbb{R}^l$, and $\hat{x}(t) \in \mathbb{R}^m$, which belong to the set of real numbers \mathbb{R}^p . These are the state of the observer, the estimated unknown input, and the estimated state vector. The matrices: $N_i \in \mathbb{R}^{m \times m}$, $G_i \in \mathbb{R}^{m \times k}$, $L_i \in \mathbb{R}^{m \times p}$, $H_i \in \mathbb{R}^{m \times l}$, $M \in \mathbb{R}^{m \times p}$,

and $\Phi_i \in \mathbb{R}^{l \times p}$, are unknown and need to be calculated for the PI observer. The estimation error is defined as:

$$e(t) = x(t) - \hat{x}(t). \quad (12)$$

By replacing $\hat{x}(t)$ from (11):

$$e(t) = x(t) - Z(t) - MCx(t) = (I_n - MC)x(t) - Z(t), \quad (13)$$

where I_n is an identity matrix of dimension n . A real matrix $U \in \mathbb{R}^{n \times n}$ is defined such that:

$$UE = I_n - MC, \quad (14)$$

which can be written as

$$[U \ M] = \begin{bmatrix} E \\ C \end{bmatrix}^+, \quad (15)$$

the superscript $+$ represents the inverse generalized matrix. From (15) the particular solution for matrices U and M is:

$$U = \begin{bmatrix} E \\ C \end{bmatrix}^+ \begin{bmatrix} I_n \\ 0 \end{bmatrix}, \quad (16)$$

$$M = \begin{bmatrix} E \\ C \end{bmatrix}^+ \begin{bmatrix} 0 \\ I_p \end{bmatrix}. \quad (17)$$

Suppose that the unknown inputs are bounded, and their dynamics are relatively slow, meaning that their time derivatives are approximately zero, i.e., $\dot{d}(t) \simeq 0$. It is important to note that we are not considering sensor bias faults in this scenario. Now, define $\delta(t)$ as:

$$\delta(t) = d(t) - \hat{d}(t), \quad (18)$$

With this definition, the derivative of $\delta(t)$ is:

$$\dot{\delta}(t) = -\dot{\hat{d}}(t) = \sum_{i=1}^{2^J} \varepsilon_i(\rho(t)) (-\Phi_i C) e(t). \quad (19)$$

The estimation error (13) can be rewritten as:

$$e(t) = UEx(t) - Z(t). \quad (20)$$

The dynamic estimation error can be written by using (1), (9), and (18) as follows:

$$\dot{e}(t) = \sum_{i=1}^{2^J} \varepsilon_i(\rho(t)) \left(N_i e(t) + (UA_i - N_i UE - L_i C)x(t) + (UB_i - G_i)u(t) + (UR_i - H_i)d(t) + H_i \delta(t) \right), \quad (21)$$

If the following conditions are verified

$$UA_i - N_i UE - L_i C = 0, \quad (22)$$

$$UB_i - G_i = 0, \quad (23)$$

$$UR_i - H_i = 0, \quad (24)$$

then, the derivative of the error is simplified to:

$$\dot{e}(t) = \sum_{i=1}^{2^J} \varepsilon_i(\rho(t)) (N_i e(t) + H_i \delta(t)). \quad (25)$$

A matrix representation of (19) and (25) is:

$$\begin{bmatrix} \dot{e}(t) \\ \dot{\delta}(t) \end{bmatrix} = \sum_{i=1}^{2^J} \varepsilon_i(\rho(t)) \begin{bmatrix} N_i & H_i \\ -\Phi_i C & 0 \end{bmatrix} \begin{bmatrix} e(t) \\ \delta(t) \end{bmatrix}. \quad (26)$$

If $Re\lambda_i \begin{bmatrix} N_i & H_i \\ -\Phi_i C & 0 \end{bmatrix} < 0$, the state estimation error and the unknown input dynamic error established in (26) converge asymptotically to zero.

Matrices G_i and H_i can be determined from equations (23) and (24) as:

$$G_i = UB_i, \quad (27)$$

$$H_i = UR_i, \quad (28)$$

where matrix U is defined in (16), and matrices B_i and R_i can be obtained from the model (1).

From (22), and condition (14), matrix N_i can be defined as:

$$N_i = UA_i - K_i C, \quad (29)$$

where $K_i = L_i - N_i M$.

By replacing (29) in (26), the state estimation error (26) can be rewritten as:

$$\underbrace{\begin{bmatrix} \dot{e}(t) \\ \dot{\delta}(t) \end{bmatrix}}_{\dot{\beta}(t)} = \sum_{i=1}^{2^J} \varepsilon_i(\rho(t)) (\bar{A}_i - \bar{K}_i \bar{C}) \underbrace{\begin{bmatrix} e(t) \\ \delta(t) \end{bmatrix}}_{\beta(t)}, \quad (30)$$

where $\bar{A}_i = \begin{bmatrix} UA_i & H_i \\ 0 & 0 \end{bmatrix}$, $\bar{K}_i = \begin{bmatrix} K_i \\ \Phi_i \end{bmatrix}$, and $\bar{C} = [C \ 0]$.

In order to implement the PI observer for a descriptor LPV system with unknown inputs, it is necessary to ensure that the pairs (\bar{A}_i, \bar{C}) are detectable for all $i = 1, 2, \dots, 2^J$. If this condition is verified, then the observer exists, and the estimation error of the system converges asymptotically to zero.

B. STABILITY ANALYSIS

For stability analysis, consider the following Lyapunov function:

$$V(\beta(t)) = \beta^T(t)P\beta(t) < 0, \quad (31)$$

where $P \in \mathbb{R}^{(n+l) \times (n+l)}$ is a positive definite matrix. The derivative of $V(\beta(t))$ is given by

$$\dot{V}(\beta(t)) = \dot{\beta}^T(t)P\beta(t) + \beta^T(t)P\dot{\beta}(t), \quad (32)$$

$$= \beta^T(t)(\bar{A}_i^T P + P\bar{A}_i - \bar{C}^T \bar{K}_i^T P - P\bar{K}_i \bar{C})\beta(t), \quad (33)$$

the condition $\dot{V}(\beta(t)) < 0$ is verified if

$$(\bar{A}_i^T P + P\bar{A}_i - \bar{C}^T \bar{K}_i^T P - P\bar{K}_i \bar{C}) < 0, \quad (34)$$

which can be written as:

$$(\bar{A}_i^T P + P\bar{A}_i - \bar{C}^T W_i^T - W_i \bar{C}) < 0, \quad (35)$$

where $W_i = P\bar{K}_i$.

The observer is asymptotically stable if there exists a positive definite symmetric matrix P , and matrices $W_i = P\bar{K}_i$ such that the Linear Matrix Inequality (LMI's) presented in (35) holds.

The observer gains can be calculated by using the expression $\bar{K}_i = P^{-1}W_i$. This calculation is important for ensuring the stability and convergence of the observation error. In order to guarantee these properties, a bounded area S can be defined in the left part of the complex plane. This area is defined by a line of abscissa $(-\sigma)$, where σ is a positive real number. To satisfy the stability and convergence requirements, the LMI's defined in (35) can be written as:

$$(\bar{A}_i^T P + P\bar{A}_i - \bar{C}^T W_i^T - W_i \bar{C}) + 2\sigma P < 0, \quad \forall i \in 1, 2, \dots, 2^J. \quad (36)$$

consequently $\hat{x}(t)$ will asymptotically converge to $x(t)$ and $\hat{d}(t)$ to $d(t)$.

C. DISTILLATION COLUMN MODEL

In order to ensure the efficient operation of a distillation column, it is essential to have a thorough understanding of its dynamic properties. This requires a deep comprehension of the steady-state behavior of the column. Moreover, to carry out the distillation process successfully, it is crucial to have knowledge about the correlations between vapor and liquid equilibrium or to estimate them accurately. These correlations play a vital role in determining the behavior of the distillation column since they are non-linear functions of temperature, pressure, and composition. Therefore, to model the behavior of the distillation column accurately, it is necessary to consider these assumptions when formulating the model [39], [40]:

- (A1) The process is an isobaric system.
- (A2) There exists an ideal liquid-vapor equilibrium.
- (A3) Non-linear mixture behavior of liquids is considered.
- (A4) The molar vapor holdup is negligible with respect to the molar liquid holdup.
- (A5) The boiler is a theoretical tray.
- (A6) The condenser is total.
- (A7) The liquid volumetric hold-up is constant.

The non-ideality of the liquid phase, known as the nonlinear characteristic, is a prevalent phenomenon in chemical systems operating at low pressure. Hence, specific models are employed to represent these non-idealities accurately. The vapor composition y_i of the desired component can be expressed by an equation that is suitable for low-pressure systems:

$$y_i(t)P_T\Phi_i = P_i^{sat}x_i(t)\gamma_i \quad (i = 1, 2, \dots, N), \quad (37)$$

where P_T is the total pressure, Φ_i is the fugacity coefficient, P_i^{sat} is the vapor partial pressure, x_i is the liquid composition, the subscript i denotes the component number in the mixture and γ_i is the activity coefficient of the component in each stage. This correction factor is highly dependent on

the concentration and can be determined using any of the six popular expressions: Margules, Van Laar, Wilson, NRTL, UNIFAC, and UNIQUAC. In this work, the vapor composition is calculated as a function of the light component (ethanol) using the Van Laar equation:

$$\begin{aligned} \ln \gamma_{EOH} &= A_{12} \left(\frac{A_{21}(1-x(t))}{A_{12}x(t) + A_{21}(1-x(t))} \right)^2, \\ \ln \gamma_{H_2O} &= A_{21} \left(\frac{A_{12}x(t)}{A_{12}x(t) + A_{21}(1-x(t))} \right)^2, \end{aligned} \quad (38)$$

where A_{12} , and A_{21} are two interaction parameters established for a binary mixture. These values depend on the mixture and can be found in [41], $A_{12} = 1.6798$, and $A_{21} = 0.9227$; the subscripts EOH and H_2O denote ethanol and water, respectively.

The model of the distillation column is divided into four basic models: the condenser x_1 , a tray x_p , the feeding tray x_F , and the boiler x_N . Column stages are labeled using an ascendant numeration from the condenser to the boiler; p denotes the tray index. By taking into account the assumptions (A1) to (A7), a set of differential equations can be derived from the balance equation on each tray for one component:

$$\begin{cases} M_1 \frac{d(x_1(t))}{dt} = V_R y_2 - L_R x_1 - D x_1, \\ M_p \frac{d(x_p(t))}{dt} = V_R (y_{p+1} - y_p) + L_R (x_{p-1} - x_p), \\ \text{with } p = 2, \dots, F-1, \\ M_F \frac{d(x_F(t))}{dt} = V_R (y_{F+1} - y_F) + L_R (x_{F-1} - x_F) + F(z_F), \\ M_p \frac{d(x_p(t))}{dt} = V_S (y_{p+1} - y_p) + L_S (x_{p-1} - x_p), \\ \text{with } p = F+1, \dots, N-1, \\ M_N \frac{d(x_N(t))}{dt} = L_S x_{N-1} - V_S y_N - B x_N, \end{cases} \quad (39)$$

The molar feeding flow and composition are represented by F , and z_F , respectively, the perturbation variables. The distilled and bottom products are denoted by D , and B . V_R , L_R , V_S , and L_S refer to the vapor and liquid molar flow on the rectifying and the stripping sections. Each tray has a molar holdup, denoted by M_p , with a total of N trays.

D. MOLAR FLOW RATES

In the distillation column exist six molar flow rates, vapor and liquid (V_S , V_R , L_S , L_R , B , and D). The vapor molar flow can be divided in V_S and V_R , depending on the stage:

$$V_S(t) = \frac{Q_b(t)}{\lambda_{EOH} x_N(t) + \lambda_{H_2O} (1 - x_N(t))}, \quad (40)$$

$$V_R(t) = V_S(t) + (1 - q_F)F(t), \quad (41)$$

where Q_b is the heating power on the boiler, λ is the vaporization enthalpy. The molar flow of the feed F is calculated by:

$$F(t) = F_V [\rho_{EOH} \omega_{EOH} + \rho_{H_2O} (1 - \omega_{EOH})]$$

$$\times \left(\frac{z_F(t)}{MW_{EOH}} + \frac{1 - z_F(t)}{MW_{H_2O}} \right). \quad (42)$$

F_V is the volumetric flow of the feeding stream, ρ_{EOH} , ρ_{H_2O} are densities for each component, and MW_{EOH} , MW_{H_2O} are molecular weights. ω_{EOH} is the weight fraction of the light component given by:

$$\omega_{EOH} = \frac{z_F(t) \rho_{EOH}}{z_F(t) \rho_{EOH} + (1 - z_F(t)) \rho_{H_2O}}. \quad (43)$$

The liquid molar flow can be calculated as:

$$\begin{aligned} L_R(t) &= (1 - r_v(t))V_R(t), \\ L_S(t) &= L_R(t) + q_F F(t), \end{aligned} \quad (44)$$

where

$$q_F = 1 + \frac{C_p(T_b - T_F)}{\lambda}, \quad (45)$$

q_F describes the feeding condition according to its vaporization degree. In (45), C_p is the specific heat, T_b is the boiling temperature, T_F is the feeding temperature, and λ is the vaporization enthalpy (in this case it is considered constant).

The r_v is a binary variable representing the reflux valve position (a three-way ON-OFF solenoid valve), i.e., $r_v = 0$ means that $L_R = V_R$, and if $r_v = 1$, then $L_R = 0$.

For this reason, the reflux R is considered as a variable percentage, and it is obtained from the relation between the opening and closing time of valve r_v (a modulation of reflux signal as a function of time).

The distilled and bottom product flow rates are:

$$\begin{aligned} D(t) &= r_v(t)V_R(t), \\ B(t) &= (L_S(t) - V_S(t))b_v, \end{aligned} \quad (46)$$

where b_v is a binary variable representing the bottom valve opening, i.e., $b_v = 0$ means that a batch distillation is performed, and if $b_v = 1$, then the bottom product B is withdrawn from the boiler.

Fig. 1 depicts a distillation column consisting of five plates. The liquid compositions are denoted from x_1 to x_5 , starting from the condenser to the boiler, respectively. The feed plate, x_3 , is positioned at the center of the column, where the feed flow F and the liquid feed composition z_F are introduced. The feed flow is derived from the feed tank FT and is pumped by the feed pump FP . Before entering the column, F passes through the electric preheating resistance $J1$, which has a power of 500W. Finally, F is admitted into the column by activating the valve $V1$.

The condenser is located at the top of the column. The solenoid reflux valve r_v opens periodically to obtain the distillate D and the reflux R . The ethanol-water mixture is placed in the boiler, heated by the electric resistance $J2$ with a heating power on the boiler Q_b of 2500W. The bottom product B is extracted by actuating the valve b_v .

The dynamic model of industrial columns is typically very large, and even the simplest dynamic model for a distillation column is complex due to the high number of nonlinear differential equations that must match the number

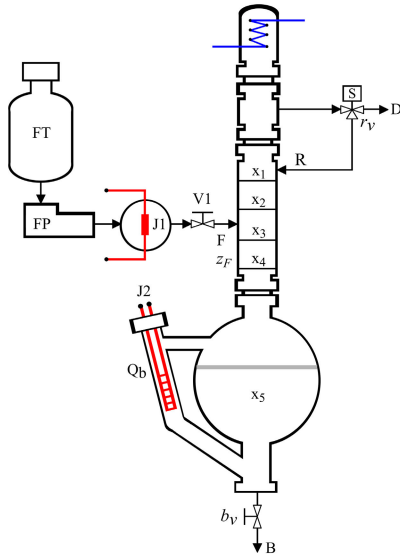


FIGURE 1. Scheme of a distillation column of five trays. The principal parts are the condenser, generic trays in the rectifying zone, generic trays in the stripping zone, feed tray, distillate product, boiler, and bottom product.

TABLE 1. Variables and initial conditions of the distillation column process.

Symbol	Value	Description
A_{12}	1.6798	Van Laar constant for ethanol-water mixture
A_{21}	0.9227	Van Laar constant for ethanol-water mixture
λ_{EOH}	38.56	vaporization enthalpy of ethanol (kJ/mol)
λ_{H_2O}	40.65	vaporization enthalpy of water (kJ/mol)
ρ_{EOH}	0.789	density of ethanol (g/cm ³)
ρ_{H_2O}	1	density of water (g/cm ³)
MW_{EOH}	46.069	molecular weight of ethanol (g/mol)
MW_{H_2O}	18.015	molecular weight of water (g/mol)
z_F	0.47	liquid feed composition (mol)
F	1	liquid flow rate of the feed (mol/s)
N	5	total of trays
x_F	3	feeding tray number
M_1	0.0736	condenser liquid holdup (mol)
M_p	0.6941	generic tray liquid holdup (mol)
M_N	189.48	bottom liquid holdup (mol)
V_S	1.72	vapor flow on the stripping section (mol/s)
V_R	1.72	vapor flow on the rectifying section (mol/s)
L_S	1.1	liquid flow on the stripping section (mol/s)
L_R	1.1	liquid flow on the rectifying section (mol/s)
q_F	1	feeding condition
B	0	bottom product flow rate (mol/s)
D	0	distillate product flow rate (mol/s)
b_v	0	bottom valve position
r_v	0	reflux valve position
x_1	0.7058	liquid composition of the distillate product (mol)
x_N	0.2565	liquid composition of the bottom product (mol)

of column plates. However, the complexity can be reduced by considering the time scales. This paper simplifies the nonlinear model of a binary distillation column, preserving the dynamics and physical properties as a descriptor model.

E. BINARY DISTILLATION COLUMN SINGULAR MODEL

Fault diagnosis and control strategies can be achieved using descriptor models, such as the works presented in [42] and [43]. The proposed simplified representation of a binary distillation column preserves the physical properties and dynamics of the plant. By considering the assumptions (A1) to (A7) mentioned before and analyzing the dynamics of

the plant depicted in Fig. 1, the equations that describe the balance for each component can be obtained, as is shown in (39).

Consider the descriptor system:

$$\begin{aligned} E\dot{x}(t) &= Ax(t) + Bu(t) + Rd(t), \\ y(t) &= Cx(t), \end{aligned} \quad (47)$$

where $E \in \mathbb{R}^{m \times m}$ is a singular matrix with $\text{rank}(E) = r < n$, $x(t) \in \mathbb{R}^m$ is the descriptor state vector; $u(t) \in \mathbb{R}^k$, and $y(t) \in \mathbb{R}^p$ are the control input and measurement output vectors, respectively; $d(t) \in \mathbb{R}^l$ is a bounded vector representing process disturbances that act as unknown inputs for the observer; A , B , R , and C are matrices with appropriate dimensions.

For the distillation column model $x = [x_1, x_2, \dots, x_N]^T$ is the state vector that represents the liquid concentrations of the light component, $u(t) = [L(t) V(t)]^T$ is the input vector. Typically, $F(t)$ and $z_F(t)$ are considered as disturbances in a distillation process, then $d(t) = [F(t) z_F(t)]^T$. By taking into account the dynamics of the plant, the system (39) can be rewritten as $\bar{x} = f(x, L, V, F, z_F)$. According to [8], f is linear with respect to L , V , F , and z_F , so it is assumed that L , V , F , and z_F are continuous in time, i.e., $t \in [0, +\infty)$ s.t. $\forall t, L(t) < V(t) < (L(t) + F(t))$. Therefore, it is possible to establish that for each L , V , F , and z_F there exists a unique steady-state $\bar{x}(t) \in [0, 1]$ namely a unique solution of $f(\bar{x}, L, V, F, z_F) = 0$. Moreover, if L , V , F , and z_F are assumed to be constant, and if $x(0) \in [0, 1]$, then the system is Lyapunov stable and its solution converges to the unique steady state associated to L , V , F , and z_F .

According to this, the model in (39) can be reduced by time scale considerations, described by the differential-algebraic system as:

$$\begin{aligned} \tilde{M}_1 \dot{x}_1 &= Vk(x_2) - Vx_1, \\ 0 &= Lx_{p-1} + Vk(x_{p+1}) - Lx_p - Vk(x_p), \\ p &= 2, \dots, j_R - 1, \\ \tilde{M}_{pR} \dot{x}_{pR} &= Lx_{pR-1} + Vk(x_{pR+1}) - Lx_{pR} - Vk(x_{pR}), \\ 0 &= Lx_{p-1} + Vk(x_{p+1}) - Lx_p - Vk(x_p), \\ p &= p_R + 1, \dots, p_F - 1, \\ \tilde{M}_{pF} \dot{x}_{pF} &= Lx_{pF-1} + Vk(x_{pF+1}) - (L + F)x_{pF} \\ &\quad - Vk(x_{pF}) + F(z_F), \\ 0 &= (L + F)x_{p-1} + Vk(x_{p+1}) - (L + F)x_p \\ &\quad - Vk(x_p), \\ p &= p_F + 1, \dots, p_S - 1, \\ \tilde{M}_{pS} \dot{x}_{pS} &= (L + F)x_{pS-1} + Vk(x_{pS+1}) - (L + F)x_{pS} \\ &\quad - Vk(x_{pS}), \\ 0 &= (L + F)x_{p-1} + Vk(x_{p+1}) - (L + F)x_p \\ &\quad - Vk(x_p), \\ p &= p_S + 1, \dots, N - 1, \\ \tilde{M}_N \dot{x}_N &= (L + F)x_{N-1} - (L + F - V)x_N - Vk(x_N). \end{aligned} \quad (48)$$

The molar holdups of the reduced model (48), are defined as follows:

$$\begin{aligned} \tilde{M}_1 &= M_1, \tilde{M}_{pR} = \sum_2^{pR} M_p, \tilde{M}_{pF} = \sum_{pR+1}^{pS-1} M_p, \\ \tilde{M}_{pS} &= \sum_{pS}^{N-1} M_p, \tilde{M}_N = M_N. \end{aligned} \quad (49)$$

The equilibrium function k is obtained by linearizing the Vapour-liquid Equilibrium (VLE) on each stage, calculated as $k_i = \Delta y_i / \Delta x_i$. The descriptor model obtained through the linearization of the process is depicted in matrices (50). The substitution of the algebraic equations into the differential equations preserves the tridiagonal structure of the original system and gives a reduced-order model.

$$\begin{aligned} E &= \begin{bmatrix} \tilde{M} & 0 & 0 & 0 & 0 \\ 0 & 0 & 0 & 0 & 0 \\ 0 & 0 & \tilde{M}_{pF} & 0 & 0 \\ 0 & 0 & 0 & 0 & 0 \\ 0 & 0 & 0 & 0 & \tilde{M}_N \end{bmatrix}, x = \begin{bmatrix} x_1 \\ x_2 \\ x_3 \\ x_4 \\ x_5 \end{bmatrix}, \\ u &= \begin{bmatrix} L \\ V \end{bmatrix}, d = \begin{bmatrix} F \\ z_F \end{bmatrix}, C = \begin{bmatrix} 0 & 1 & 0 & 0 & 0 \\ 0 & 0 & 0 & 1 & 0 \end{bmatrix}, \\ A &= \begin{bmatrix} -L_R - D & V_R k_2 & 0 & 0 \\ L_R & -L_R - (V_R k_2) & V_R k_3 & 0 \\ 0 & L_R & -L_S - (V_R k_3) & V_S k_4 \\ 0 & 0 & L_S & -L_S - (V_S k_4) \\ 0 & 0 & 0 & L_S \\ & 0 & & & \\ & 0 & & & \\ & 0 & & & \\ & V_S k_5 & & & \\ -L_S - (V_S k_5) + V_S - B & & & & \end{bmatrix}, \\ B &= \begin{bmatrix} 0 & 0 \\ x_1 - x_2 & k_3 x_3 - k_2 x_2 \\ x_2 - x_3 & k_4 x_4 - k_3 x_3 \\ x_3 - x_4 & k_5 x_5 - k_4 x_4 \\ x_4 - x_5 & x_5 - k_5 x_5 \end{bmatrix}, R = \begin{bmatrix} 0 & 0 \\ 0 & 0 \\ z_F - x_3 & F \\ x_3 - x_4 & 0 \\ x_4 - x_5 & 0 \end{bmatrix}, \end{aligned} \quad (50)$$

After this, the descriptor model is described as a multi-linear descriptor system in which the system matrices are set by known operation points. In this case, the system (47) is represented as a descriptor LPV system with a polytopic form when the parameters evolve in a polytopic domain:

$$\begin{aligned} E \dot{x}(t) &= \sum_{i=1}^{2^J} \varepsilon_i(\rho(t)) [A_i x(t) + B_i u(t) + R_i d(t)], \\ y(t) &= C x(t), \end{aligned} \quad (51)$$

where $A_i \in \mathbb{R}^{m \times m}$, $B_i \in \mathbb{R}^{m \times k}$, $R_i \in \mathbb{R}^{m \times l}$, and $C \in \mathbb{R}^{p \times m}$ are known constants matrices.

The parameter vector $\rho(t) = [\rho_1(t), \dots, \rho_J(t)]$ varies in a convex polytope with 2^J vertices, J denotes the total number

of parameters. The polytope is a hypercube of dimension 2^J whose vertices or submodels are combined by the $\varepsilon_i(\rho(t))$ weighting functions to yield a global model, with $i = 1, 2, \dots, 2^J$. These functions are defined by:

$$\begin{aligned} \varepsilon_1(\rho(t)) &= \frac{(\rho_1 - \underline{\rho}_1)(\rho_2 - \underline{\rho}_2)}{(\bar{\rho}_1 - \underline{\rho}_1)(\bar{\rho}_2 - \underline{\rho}_2)}, \\ \varepsilon_2(\rho(t)) &= \frac{(\rho_1 - \underline{\rho}_1)(\bar{\rho}_2 - \rho_2)}{(\bar{\rho}_1 - \underline{\rho}_1)(\bar{\rho}_2 - \underline{\rho}_2)}, \\ \varepsilon_3(\rho(t)) &= \frac{(\bar{\rho}_1 - \rho_1)(\rho_2 - \underline{\rho}_2)}{(\bar{\rho}_1 - \underline{\rho}_1)(\bar{\rho}_2 - \underline{\rho}_2)}, \\ \varepsilon_4(\rho(t)) &= \frac{(\bar{\rho}_1 - \rho_1)(\bar{\rho}_2 - \rho_2)}{(\bar{\rho}_1 - \underline{\rho}_1)(\bar{\rho}_2 - \underline{\rho}_2)}, \end{aligned} \quad (52)$$

where $\varepsilon_i(\rho(t)) = \varepsilon(\bar{\rho}, \underline{\rho}, \rho(t), t)$ with $\bar{\rho}$ and $\underline{\rho}$ representing the maximum and the minimum value of $\rho(t)$, respectively. These functions lie in the convex set as follows:

$$\Theta = \left\{ \begin{aligned} &\varepsilon_i(\rho(t)) \in \mathbb{R}^{2^J}, \varepsilon_i(\rho) = [\varepsilon_1(\rho), \dots, \varepsilon_{2^J}(\rho)]^T, \\ &\varepsilon_i(\rho) \geq 0, \forall i, \sum_{i=1}^{2^J} \varepsilon_i(\rho(t)) = 1, \end{aligned} \right\}. \quad (53)$$

The expression in (51) defines a system that can be represented as a continuous-time polytopic descriptor LPV system, as outlined in (1), with the parameter $\rho(t)$ varying within a convex polytope characterized by vertices 2^J . In this context, the model can be regarded as a multi-linear system, with the system matrices being determined by the known operating points, as described in [42].

III. SIMULATIONS RESULTS

The general scheme of a distillation column is illustrated in Fig. 1. The simulation is conducted using a five-tray distillation column. Temperature sensors are positioned within the main body of the column, specifically on plates 2 and 4. The liquid compositions can be obtained using these measurements and considering the liquid-vapor equilibrium relation. The mixture used in these simulations is ethanol (EOH) and water (H₂O) which is considered a non-ideal mixture. The physical specifications of the components of the binary mixture are presented in Table 1.

The simulation of the model given in (51) is done considering: EOH volume of 2000 ml, H₂O volume of 2000 ml and process total pressure of 105.86 kPa. The distillation column is operated under LV configuration; this implies that inputs or manipulated variables are the reflux (R) and the heating power on the boiler (Q_b). The reflux R is considered a variable percentage, and it is obtained from the relation between the opening and closing time of valve r_v (a modulation of reflux signal as a function of time). The outputs or controlled variables are the top product composition (x_1) and the bottom product composition (x_N).

The model for the binary distillation column considers four operational points reached by adjusting the reflux valve r_v and

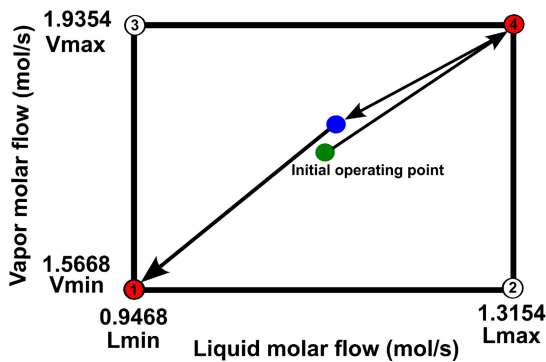


FIGURE 2. The convex polytope is represented by 2^J vertices or submodels at the corners and designated from 1 to 4. The green middle point denotes the initial operation point, and the black arrows indicate the trajectory of the parameters within the polytope.

the heating power on the boiler Q_b . This adjustment leads to changes in the molar flows, which, in turn, produces different concentrations of ethanol that can be obtained during the distillation process.

Fig. 2 displays the convex polytope generated by considering $J = 2$ parameters. The first parameter is the liquid flow on the rectifying section (mol/s), denoted as $\rho_1(t) = L_R$, is in the range of 0.9468 mol/min and 1.3154 mol/min. It is determined by controlling the reflux valve r_v . The minimum value is obtained when r_v is turned off, while the maximum value is obtained when r_v is a pulse width modulated flow signal (turned on for $t_{ON} = 6s$ and turned off for $t_{OFF} = 6s$). The second parameter is the vapor flow on the stripping section (mol/s), denoted as $\rho_2(t) = V_S$, is in the range of 1.5668 mol/min and 1.9354 mol/min. It is manipulated by adjusting the heating power on the boiler Q_b , which is controlled by the electric resistance $J2$. The minimum heating power is 650W, whereas the maximum is 2500W.

An observer is designed to determine the ethanol composition in each tray by using a model that describes the VLE of the binary mixture of ethanol and water, the initial conditions of the observer are $\hat{x}^0(t) = [0.5, 0.4, 0.3, 0.2, 0.1]^T$. A five-plate distillation column is considered. The initial conditions of states are $x^0(t) = [0.7058, 0.6199, 0.4053, 0.3711, 0.2565]^T$. Temperature sensors are placed on plates 2 and 4; the liquid compositions can be obtained using these measurements and considering the equilibrium relation.

The nonlinear dynamic system is represented in a descriptor LPV form by a set of matrices, by considering four operation points based on the minimum and maximum values of parameters $\rho_1(t)$ and $\rho_2(t)$ as follows:

$$E = \begin{bmatrix} 0.073 & 0 & 0 & 0 & 0 \\ 0 & 0 & 0 & 0 & 0 \\ 0 & 0 & 2.08 & 0 & 0 \\ 0 & 0 & 0 & 0 & 0 \\ 0 & 0 & 0 & 0 & 189.48 \end{bmatrix}, \quad C = \begin{bmatrix} 0 & 1 & 0 & 0 & 0 \\ 0 & 0 & 0 & 1 & 0 \end{bmatrix},$$

$$A_1 = \begin{bmatrix} -1.9354 & 2.2216 & 0 & 0 & 0 \\ 0.9468 & -3.1684 & 2.4797 & 0 & 0 \\ 0 & 0.9468 & -4.4265 & 2.7913 & 0 \\ 0 & 0 & 1.9468 & -4.7381 & 4.2455 \\ 0 & 0 & 0 & 1.9468 & -4.2569 \end{bmatrix},$$

$$B_1 = \begin{bmatrix} 0 & 0 \\ 0.0903 & -0.0442 \\ 0.0980 & -0.0261 \\ 0.0753 & -0.0757 \\ 0.1842 & -0.3018 \end{bmatrix}, \quad R_1 = \begin{bmatrix} 0 & 0 \\ 0 & 0 \\ -0.0424 & 1 \\ 0.0753 & 0 \\ 0.1842 & 0 \end{bmatrix},$$

$$A_2 = \begin{bmatrix} -1.5668 & 1.7686 & 0 & 0 & 0 \\ 0.9468 & -2.7154 & 1.9655 & 0 & 0 \\ 0 & 0.9468 & -3.9123 & 2.1737 & 0 \\ 0 & 0 & 1.9468 & -4.1205 & 3.4688 \\ 0 & 0 & 0 & 1.9468 & -3.8488 \end{bmatrix},$$

$$B_2 = \begin{bmatrix} 0 & 0 \\ 0.0812 & -0.0491 \\ 0.1023 & -0.0247 \\ 0.0684 & -0.0850 \\ 0.2100 & -0.3032 \end{bmatrix}, \quad R_2 = \begin{bmatrix} 0 & 0 \\ 0 & 0 \\ -0.0582 & 1 \\ 0.0684 & 0 \\ 0.2100 & 0 \end{bmatrix},$$

$$A_3 = \begin{bmatrix} -1.5668 & 1.7225 & 0 & 0 & 0 \\ 1.3154 & -3.0379 & 1.8830 & 0 & 0 \\ 0 & 1.3154 & -4.1984 & 2.0484 & 0 \\ 0 & 0 & 2.3154 & -4.3638 & 3.4532 \\ 0 & 0 & 0 & 2.3154 & -4.2018 \end{bmatrix},$$

$$B_3 = \begin{bmatrix} 0 & 0 \\ 0.0663 & -0.0557 \\ 0.1032 & -0.0266 \\ 0.0659 & -0.0974 \\ 0.2468 & -0.3025 \end{bmatrix}, \quad R_3 = \begin{bmatrix} 0 & 0 \\ 0 & 0 \\ -0.0940 & 1 \\ 0.0659 & 0 \\ 0.2468 & 0 \end{bmatrix},$$

$$A_4 = \begin{bmatrix} -1.9354 & 2.1583 & 0 & 0 & 0 \\ 1.3154 & -3.4737 & 2.3722 & 0 & 0 \\ 0 & 1.3154 & -4.6876 & 2.6292 & 0 \\ 0 & 0 & 2.3154 & -4.9446 & 4.2669 \\ 0 & 0 & 0 & 2.3154 & -4.6469 \end{bmatrix},$$

$$B_4 = \begin{bmatrix} 0 & 0 \\ 0.0745 & -0.0506 \\ 0.0996 & -0.0280 \\ 0.0740 & -0.0986 \\ 0.2217 & -0.3026 \end{bmatrix}, \quad R_4 = \begin{bmatrix} 0 & 0 \\ 0 & 0 \\ -0.0769 & 1 \\ 0.0740 & 0 \\ 0.2217 & 0 \end{bmatrix}.$$

The matrices $N_i, L_i, G_i,$ and H_i in (22) - (24) are computed by using the Yalmip Toolbox [44]:

$$N_1 = \begin{bmatrix} -1.9354 & 0.4211 & 0 & -0.7609 & 0 \\ 0 & -2.6432 & 0 & -1.4938 & 0 \\ 0 & -0.2336 & -4.4265 & 1.2331 & 0 \\ 0 & -1.3979 & 0 & -2.5324 & 0 \\ 0 & -0.7589 & 0 & 0.5997 & -4.2569 \end{bmatrix},$$

$$N_2 = \begin{bmatrix} -1.5668 & 0.0053 & 0 & -0.7601 & 0 \\ 0 & -2.6091 & 0 & -1.4882 & 0 \\ 0 & -0.2365 & -3.9123 & 0.6418 & 0 \\ 0 & -1.4055 & 0 & -2.5020 & 0 \\ 0 & -0.7620 & 0 & 0.6094 & -3.8488 \end{bmatrix},$$

$$\begin{aligned}
 N_3 &= \begin{bmatrix} -1.5668 & -0.0542 & 0 & -0.7699 & 0 \\ 0 & -2.6338 & 0 & -1.5022 & 0 \\ 0 & 0.1093 & -4.1984 & 0.5119 & 0 \\ 0 & -1.4241 & 0 & -2.5254 & 0 \\ 0 & -0.7688 & 0 & 0.9613 & -4.2018 \end{bmatrix}, \\
 N_4 &= \begin{bmatrix} -1.9354 & 0.3621 & 0 & -0.7758 & 0 \\ 0 & -2.6484 & 0 & -1.5112 & 0 \\ 0 & 0.1135 & -4.6876 & 1.0789 & 0 \\ 0 & -1.4222 & 0 & -2.5306 & 0 \\ 0 & -0.7688 & 0 & 0.9647 & -4.6469 \end{bmatrix}, \\
 L_1 &= \begin{bmatrix} 2.2216 & 0 \\ 0 & 0 \\ 0.9468 & 2.7913 \\ 0 & 0 \\ 0 & 1.9468 \end{bmatrix}, \quad L_2 = \begin{bmatrix} 1.7686 & 0 \\ 0 & 0 \\ 0.9468 & 2.1737 \\ 0 & 0 \\ 0 & 1.9468 \end{bmatrix}, \\
 L_3 &= \begin{bmatrix} 1.7225 & 0 \\ 0 & 0 \\ 1.3154 & 2.0484 \\ 0 & 0 \\ 0 & 2.3154 \end{bmatrix}, \quad L_4 = \begin{bmatrix} 2.1583 & 0 \\ 0 & 0 \\ 1.3154 & 2.6292 \\ 0 & 0 \\ 0 & 2.3154 \end{bmatrix}, \\
 G_1 &= \begin{bmatrix} 0 & 0 \\ 0 & 0 \\ 0.0980 & -0.0261 \\ 0 & 0 \\ 0.1842 & -0.3018 \end{bmatrix}, \quad G_2 = \begin{bmatrix} 0 & 0 \\ 0 & 0 \\ 0.1023 & -0.0247 \\ 0 & 0 \\ 0.2100 & -0.3032 \end{bmatrix}, \\
 G_3 &= \begin{bmatrix} 0 & 0 \\ 0 & 0 \\ 0.1032 & -0.0266 \\ 0 & 0 \\ 0.2468 & -0.3025 \end{bmatrix}, \quad G_4 = \begin{bmatrix} 0 & 0 \\ 0 & 0 \\ 0.0996 & -0.0280 \\ 0 & 0 \\ 0.2217 & -0.3026 \end{bmatrix}, \\
 H_1 &= \begin{bmatrix} 0 & 0 \\ 0 & 0 \\ -0.0424 & 1.0000 \\ 0 & 0 \\ 0.1842 & 0 \end{bmatrix}, \quad H_2 = \begin{bmatrix} 0 & 0 \\ 0 & 0 \\ -0.0582 & 1.0000 \\ 0 & 0 \\ 0.2100 & 0 \end{bmatrix}, \\
 H_3 &= \begin{bmatrix} 0 & 0 \\ 0 & 0 \\ -0.0940 & 1.0000 \\ 0 & 0 \\ 0.2468 & 0 \end{bmatrix}, \quad H_4 = \begin{bmatrix} 0 & 0 \\ 0 & 0 \\ -0.0769 & 1.0000 \\ 0 & 0 \\ 0.2217 & 0 \end{bmatrix}, \\
 K_1 &= \begin{bmatrix} 1.8005 & 0.7609 \\ 2.6432 & 1.4938 \\ 1.1804 & 1.5582 \\ 1.3979 & 2.5324 \\ 0.7589 & 1.3471 \end{bmatrix}, \quad K_2 = \begin{bmatrix} 1.7633 & 0.7601 \\ 2.6091 & 1.4882 \\ 1.1833 & 1.5319 \\ 1.4055 & 2.5020 \\ 0.7620 & 1.3374 \end{bmatrix}, \\
 K_3 &= \begin{bmatrix} 1.7767 & 0.7699 \\ 2.6338 & 1.5022 \\ 1.2061 & 1.5365 \\ 1.4241 & 2.5254 \\ 0.7688 & 1.3541 \end{bmatrix}, \quad K_4 = \begin{bmatrix} 1.7962 & 0.7758 \\ 2.6484 & 1.5112 \\ 1.2019 & 1.5503 \\ 1.4222 & 2.5306 \\ 0.7688 & 1.3507 \end{bmatrix}.
 \end{aligned}$$

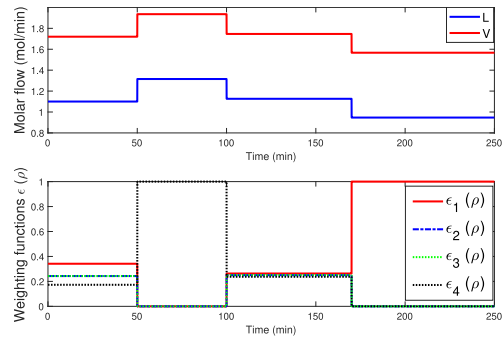


FIGURE 3. Inputs and weighting functions. Operating point changes in the molar flows L and V (top) and the weighting functions for the LPV descriptor model (bottom).

nonlinear system, including its evolution, is determined by the weighting functions $\varepsilon_i(\rho(t))$, as shown in Fig. 3 (bottom).

The weighting functions vary based on the parameter changes. A comparison of Fig. 2 and Fig. 3 reveals that the initial operating point, achieved during the stable state of the process, lies at the center of the convex polytope (indicated by the green point). The conditions of this initial operating point persist until the 50th minute, at which point the weighting functions demonstrate contributions from the four submodels or vertices of the polytope.

During the time frame of minutes 50 to 100, an adjustment in the operating point is executed, reaching the submodel 4 (identified as a red dot in the top-right section of Fig. 2). At this juncture, the complete contribution of 100% from $\varepsilon_4(\rho(t))$ is evident, as depicted by a black dotted line in Fig. 3.

In the analysis, it is essential to note that the third operating point, shown as a blue point and located in the middle part of the polytope between minutes 100 and 170, contributes to the four submodels of the polytope. Additionally, the fourth operating point, where the values of two parameters are at a minimum, corresponds to the location of submodel one. This point is represented as a red dot in the lower left part of the polytope and has a 100% contribution for the weighting function $\varepsilon_1(\rho(t))$, from minute 170 to the end of the simulation.

The proposed multi-model representation is compared with the nonlinear model. Fig. 4 shows the dynamics of the liquid compositions in the condenser, feed tray, and boiler of both models. It can be verified that both models reproduce the same process dynamics. This comparison helps in understanding the effectiveness of the modeling method used in the study and its potential applications in various fields.

Fig. 5 displays the dynamics of the process variables x_1, \dots, x_5 (green lines) and their estimation $\hat{x}_1, \dots, \hat{x}_5$ (red dotted lines), where the higher concentration corresponds to the liquid composition of the distillate product x_1 and the lower concentration corresponds to the liquid composition of the bottom product x_5 . The performance of the observer is evaluated by using the Euclidean norm of the error given in (12). The corresponding estimation errors are shown in

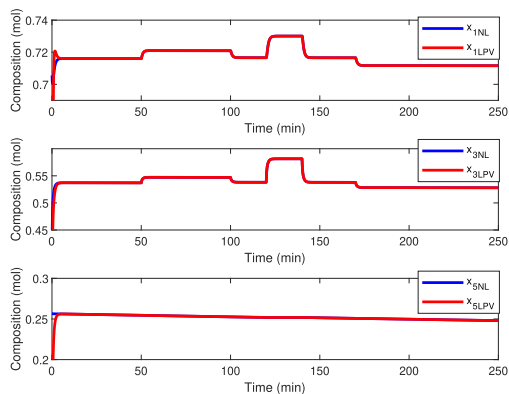


FIGURE 4. Comparison of liquid compositions for the nonlinear system and the LPV singular model, condenser x_1 (top), feed tray x_3 (middle), and boiler x_5 (bottom).

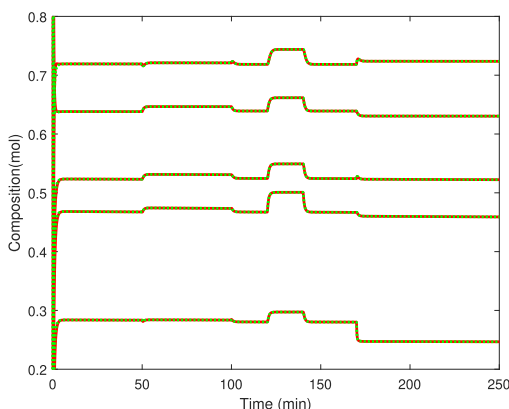


FIGURE 5. States of LPV descriptor model (green) and estimated states with the PI Observer (red).

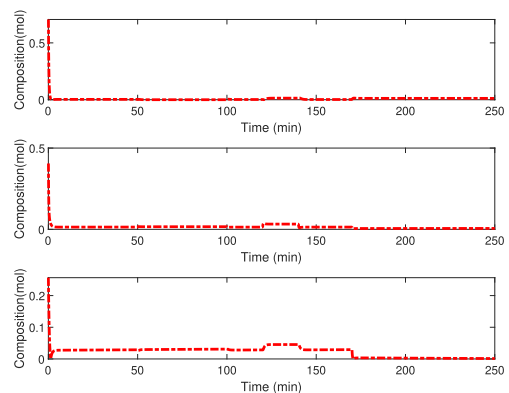


FIGURE 6. Euclidean norm of the error $e = \|x - \hat{x}\|$ for states estimation corresponding to liquid compositions in condenser x_1 (top), feed tray x_3 (middle), and boiler x_5 (bottom).

Fig. 6. It is worth noting that the observer performs well in adequately estimating the simulated process variables.

As described in subsection II-E, typically, $F(t)$ and $z_F(t)$ are considered as disturbances in a distillation process. $F(t)$, is controlled by a peristaltic pump with a stepper motor (FP in Fig. 1) and in normal process operation, it should be constant. A variation of F is considered as an abnormal operation of the plant. This variation can be caused by a fault in the peristaltic pump, a leak in the feed lines of the distillation column or an abnormal operation of the valve V1 (see Fig. 1). In order

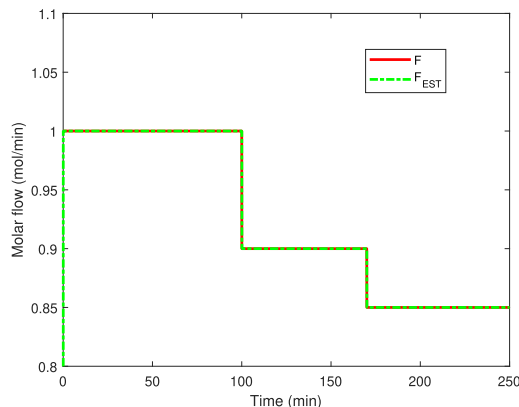


FIGURE 7. Unknown input Molar Flow F (red) and corresponding estimated (green).

to simulate an existing fault in the feeding subsystem (the peristaltic pump, a leak on the feeding lines or an abnormal opening of V1), F varies as shown in Fig. 7, beginning with a value of $F = 1$ mol/min and after that, an abnormal decreasing to $F = 0.9$ mol/min at $t = 100$ min and to $F = 0.85$ mol/min at $t = 170$ min. The estimation of F is illustrated in Fig. 7. It can be concluded that the PI observer has the ability to detect/estimate abnormal changes in the liquid flow rate of the feed.

IV. CONCLUSION

In this work, the nonlinear system of a binary distillation column is simplified to obtain a model that adequately represents the system. This simplified model is ideal for the development of state estimators.

To assess the observer’s performance, the nonlinear model of the binary distillation column is considered as a descriptor LPV system. The observer is designed to estimate both the states and the unknown input of the system. The efficiency of the observer design algorithm is evaluated through simulation experiments using the Yalmip Toolbox. Specifically, the LMI’s of (36) are solved using the Yalmip Toolbox.

The observer design approach is then applied to a nonlinear model of a five-tray binary distillation column. The observer is used to estimate the tray compositions for non-ideal mixtures. The simulation experiments demonstrate the effectiveness of the observer design approach.

Implementing the proposed method in a real-time distillation column process depends on accurately determining the polytope vertices. This method involves utilizing two parameters derived from liquid-vapor relations, which are computed based on temperature measurements from sensors positioned on plates 2 and 4 within the column. It is worth noting that the column may have a variable number of trays, and temperature data may not be accessible for every tray. Therefore, selecting trays with slow dynamics is crucial, as indicated by the modified model in (48), where the liquid molar holdups \tilde{M} are multiplied by the state variables.

It is recommended that multiple experiments be carried out to determine the vertices of the polytope and to establish the

trajectories that will conform to the parameters within the polytope.

The descriptor LPV representation involves four linear models with two parameters. The proposed model is implemented for a five-tray distillation column to approximate the nonlinear behavior of the column using simple linear models. One potential challenge of this method is determining the operating points and selecting the parameters, as they need to encompass the entire operating range of the process. This study suggests an alternative representation to the conventional model through the use of descriptor LPV systems. This model will enable the development of strategies focused on control and design for fault-tolerant control system schemes.

Future work involves developing a fault-tolerant control system specifically to address actuator faults. The objective is to implement a system that demonstrates robust and reliable performance in the management of real-world distillation column processes.

REFERENCES

- [1] R. S. Johnson, *Singular Perturbation Theory: Mathematical and Analytical Techniques With Applications to Engineering*, 1st ed, New York, NY, USA: Springer, 2005.
- [2] S. Bian and M. A. Henson, "Measurement selection for on-line estimation of nonlinear wave models for high purity distillation columns," *Chem. Eng. Sci.*, vol. 61, no. 10, pp. 3210–3222, May 2006, doi: [10.1016/j.ces.2005.11.066](https://doi.org/10.1016/j.ces.2005.11.066).
- [3] A. A. Khudhur and S. L. Jasim, "Addressing stability challenges in linear descriptor systems: A unified approach to robust control," *Results Control Optim.*, vol. 13, Dec. 2023, Art.no.100314, doi: [10.1016/j.rico.2023.100314](https://doi.org/10.1016/j.rico.2023.100314).
- [4] D. Zhang, L. D. Couto, S. Benjamin, W. Zeng, D. F. Coutinho, and S. J. Moura, "State of charge estimation of parallel connected battery cells via descriptor system theory," in *Proc. Amer. Control Conf. (ACC)*, Denver, CO, USA, 2020, pp. 2207–2212, doi: [10.23919/ACC45564.2020.9147284](https://doi.org/10.23919/ACC45564.2020.9147284).
- [5] S. Meng, F. Meng, H. Chi, H. Chen, and A. Pang, "A robust observer based on the nonlinear descriptor systems application to estimate the state of charge of lithium-ion batteries," *J. Franklin Inst.*, vol. 360, no. 16, pp. 11397–11413, Nov. 2023, doi: [10.1016/j.jfranklin.2023.08.037](https://doi.org/10.1016/j.jfranklin.2023.08.037).
- [6] P. Schmitz, A. Engelmann, T. Faulwasser, and K. Worthmann, "Data-driven MPC of descriptor systems: A case study for power networks," *IFAC-PapersOnLine*, vol. 55, no. 30, pp. 359–364, 2022, doi: [10.1016/j.ifacol.2022.11.079](https://doi.org/10.1016/j.ifacol.2022.11.079).
- [7] A. Qiu, Z. Ding, and S. Wang, "A descriptor system design framework for false data injection attack toward power systems," *Electr. Power Syst. Res.*, vol. 192, Mar. 2021, Art. no. 106932, doi: [10.1016/j.epsr.2020.106932](https://doi.org/10.1016/j.epsr.2020.106932).
- [8] J. Lévine and P. Rouchon, "Quality control of binary distillation columns via nonlinear aggregated models," *Automatica*, vol. 27, no. 3, pp. 463–480, May 1991, doi: [10.1016/0005-1098\(91\)90104-a](https://doi.org/10.1016/0005-1098(91)90104-a).
- [9] S. Bian, S. Khowinij, M. A. Henson, P. Belanger, and L. Megan, "Compartmental modeling of high purity air separation columns," *Comput. Chem. Eng.*, vol. 29, no. 10, pp. 2096–2109, Sep. 2005, doi: [10.1016/j.compchemeng.2005.06.002](https://doi.org/10.1016/j.compchemeng.2005.06.002).
- [10] A.-T. Nguyen, J. Pan, T.-M. Guerra, M. Blandeau, and W. Zhang, "Designing fuzzy descriptor observer with unmeasured premise variables for head-two-arms-trunk system," *IFAC-PapersOnLine*, vol. 53, no. 2, pp. 8007–8012, 2020, doi: [10.1016/j.ifacol.2020.12.2227](https://doi.org/10.1016/j.ifacol.2020.12.2227).
- [11] Y. Wang, X. Xie, M. Chadli, S. Xie, and Y. Peng, "Sliding-mode control of fuzzy singularly perturbed descriptor systems," *IEEE Trans. Fuzzy Syst.*, vol. 29, no. 8, pp. 2349–2360, Aug. 2021, doi: [10.1109/TFUZZ.2020.2998519](https://doi.org/10.1109/TFUZZ.2020.2998519).
- [12] R. Toth, J. C. Willems, P. S. C. Heuberger, and P. M. J. Van den Hof, "The behavioral approach to linear parameter-varying systems," *IEEE Trans. Autom. Control*, vol. 56, no. 11, pp. 2499–2514, Nov. 2011, doi: [10.1109/TAC.2011.2109439](https://doi.org/10.1109/TAC.2011.2109439).
- [13] M. Hypiúsová and D. Rosinová, "Parameter varying descriptor system control via gain scheduling," *IFAC-PapersOnLine*, vol. 52, no. 27, pp. 198–203, 2019, doi: [10.1016/j.ifacol.2019.12.756](https://doi.org/10.1016/j.ifacol.2019.12.756).
- [14] L. Chen, Y. Ding, K. Hao, and L. Ren, "An intelligent modeling approach for LPV systems based on primary-secondary response mechanism of immune system," *IFAC-PapersOnLine*, vol. 50, no. 1, pp. 5338–5342, Jul. 2017, doi: [10.1016/j.ifacol.2017.08.923](https://doi.org/10.1016/j.ifacol.2017.08.923).
- [15] D. Rotondo, F. Nejjari, and V. Puig, "Quasi-LPV modeling, identification and control of a twin rotor MIMO system," *Control Eng. Pract.*, vol. 21, no. 6, pp. 829–846, Jun. 2013, doi: [10.1016/j.conengprac.2013.02.004](https://doi.org/10.1016/j.conengprac.2013.02.004).
- [16] C. Briat, *Linear Parameter-Varying and Time-Delay Systems*. Berlin, Germany: Springer, 2015, doi: [10.1007/978-3-662-44050-6](https://doi.org/10.1007/978-3-662-44050-6).
- [17] N. Shlezinger, J. Whang, Y. C. Eldar, and A. G. Dimakis, "Model-based deep learning," in *Proc. IEEE*, vol. 111, no. 5, pp. 465–499, May 2023, doi: [10.1109/JPROC.2023.3247480](https://doi.org/10.1109/JPROC.2023.3247480).
- [18] J. Morales, J. Moeyersons, P. Armanac, M. Orini, L. Faes, S. Overeem, M. Van Gilst, J. Van Dijk, S. Van Huffel, R. Bailon, and C. Varon, "Model-based evaluation of methods for respiratory sinus arrhythmia estimation," *IEEE Trans. Biomed. Eng.*, vol. 68, no. 6, pp. 1882–1893, Jun. 2021, doi: [10.1109/TBME.2020.3028204](https://doi.org/10.1109/TBME.2020.3028204).
- [19] H. Hamdi, M. Rodrigues, B. Rabaoui, and N. Benhadj Braiek, "A fault estimation and fault-tolerant control based sliding mode observer for LPV descriptor systems with time delay," *Int. J. Appl. Math. Comput. Sci.*, vol. 31, no. 2, pp. 247–258, 2021, doi: [10.34768/amcs-2021-0017](https://doi.org/10.34768/amcs-2021-0017).
- [20] J. C. L. Chan, T. H. Lee, C. P. Tan, H. Trinh, and J. H. Park, "A nonlinear observer for robust fault reconstruction in one-sided Lipschitz and quadratically inner-bounded nonlinear descriptor systems," *IEEE Access*, vol. 9, pp. 22455–22469, 2021, doi: [10.1109/ACCESS.2021.3056136](https://doi.org/10.1109/ACCESS.2021.3056136).
- [21] C. Ríos-Ruiz, G.-L. Osorio-Gordillo, C.-M. Astorga-Zaragoza, M. Darouach, H. Souley-Ali, and J. Reyes-Reyes, "Generalized functional observer for descriptor nonlinear systems—A Takagi–Sugeno approach," *Processes*, vol. 11, no. 6, p. 1707, Jun. 2023, doi: [10.3390/pr11061707](https://doi.org/10.3390/pr11061707).
- [22] C. Wang, W. Dong, J. Wang, and Z. Ding, "Predictive descriptor observer design for a class of linear time-invariant systems with applications to quadrotor trajectory tracking," *IEEE Trans. Ind. Electron.*, vol. 68, no. 10, pp. 10019–10028, Oct. 2021, doi: [10.1109/TIE.2020.3028803](https://doi.org/10.1109/TIE.2020.3028803).
- [23] D. Koenig and S. Mammar, "Design of proportional-integral observer for unknown input descriptor systems," *IEEE Trans. Autom. Control*, vol. 47, no. 12, pp. 2057–2062, Dec. 2002, doi: [10.1109/TAC.2002.805675](https://doi.org/10.1109/TAC.2002.805675).
- [24] K. Houada, D. Saïfia, M. Chadli, and S. Labiod, "Unknown input observer based robust control for fuzzy descriptor systems subject to actuator saturation," *Math. Comput. Simul.*, vol. 203, pp. 150–173, Jan. 2023, doi: [10.1016/j.matcom.2022.06.013](https://doi.org/10.1016/j.matcom.2022.06.013).
- [25] F. Hamzaoui, M. Khadhraoui, and H. Messaoud, "Unknown input observer for linear singular systems with variable delay: The continuous and the discrete time cases," *Int. J. Model., Identificat. Control*, vol. 41, no. 3, p. 193, Dec. 2022, doi: [10.1504/ijmic.2022.127517](https://doi.org/10.1504/ijmic.2022.127517).
- [26] D. Koenig, "Observer design for unknown input nonlinear descriptor systems via convex optimization," *IEEE Trans. Autom. Control*, vol. 51, no. 6, pp. 1047–1052, Jun. 2006, doi: [10.1109/TAC.2006.876807](https://doi.org/10.1109/TAC.2006.876807).
- [27] L.-W. Liu, W. Xie, and L.-W. Zhang, "Luenberger-type interval observer for continuous-time perturbed singular systems," *Syst. Control Lett.*, vol. 173, Mar. 2023, Art.no.105484, doi: [10.1016/j.sysconle.2023.105484](https://doi.org/10.1016/j.sysconle.2023.105484).
- [28] J. Chen, J. Yu, and H.-K. Lam, "Adaptive fuzzy tracking control for a class of singular systems via output feedback scheme," *IEEE Trans. Fuzzy Syst.*, vol. 30, no. 3, pp. 610–622, Mar. 2022, doi: [10.1109/TFUZZ.2020.3042615](https://doi.org/10.1109/TFUZZ.2020.3042615).
- [29] T.-K. Yeu, H.-S. Kim, and S. Kawaji, "Fault detection, isolation and reconstruction for descriptor systems," *Asian J. Control*, vol. 7, no. 4, pp. 356–367, Oct. 2008, doi: [10.1111/j.1934-6093.2005.tb00398.x](https://doi.org/10.1111/j.1934-6093.2005.tb00398.x).
- [30] H. Hamdi, M. Rodrigues, C. Mechmeche, D. Theilliol, and N. B. Braiek, "State estimation for polytopic LPV descriptor systems: Application to fault diagnosis," *IFAC Proc. Volumes*, vol. 42, no. 8, pp. 438–443, 2009, doi: [10.3182/20090630-4-es-2003.00073](https://doi.org/10.3182/20090630-4-es-2003.00073).
- [31] G. Ortiz-Torres, J. E. Valdez-Resendiz, C. A. Torres-Cantero, J. Y. Rumbo-Morales, M. B. Ramos-Martinez, and J. S. Valdez-Martinez, "Actuator and sensor fault detection and isolation system applied to a distillation column," *IEEE Access*, vol. 11, pp. 48548–48558, 2023, doi: [10.1109/ACCESS.2023.3276717](https://doi.org/10.1109/ACCESS.2023.3276717).

- [32] Z. Zuo, D. W. C. Ho, and Y. Wang, "Fault tolerant control for singular systems with actuator saturation and nonlinear perturbation," *Automatica*, vol. 46, no. 3, pp. 569–576, Mar. 2010, doi: [10.1016/j.automatica.2010.01.024](https://doi.org/10.1016/j.automatica.2010.01.024).
- [33] P. Li, A.-T. Nguyen, H. Du, Y. Wang, and H. Zhang, "Polytopic LPV approaches for intelligent automotive systems: State of the art and future challenges," *Mech. Syst. Signal Process.*, vol. 161, Dec. 2021, Art. no. 107931, doi: [10.1016/j.ymssp.2021.107931](https://doi.org/10.1016/j.ymssp.2021.107931).
- [34] D. Ichalal, B. Marx, J. Ragot, and D. Maquin, "Fault diagnosis for Takagi–Sugeno nonlinear systems," *IFAC Proc. Volumes*, vol. 42, no. 8, pp. 504–509, 2009, doi: [10.3182/20090630-4-es-2003.00084](https://doi.org/10.3182/20090630-4-es-2003.00084).
- [35] J. Han, X. Liu, X. Wei, and X. Hu, "Adaptive adjustable dimension observer based fault estimation for switched fuzzy systems with unmeasurable premise variables," *Fuzzy Sets Syst.*, vol. 452, pp. 149–167, Jan. 2023, doi: [10.1016/j.fss.2022.06.017](https://doi.org/10.1016/j.fss.2022.06.017).
- [36] J. Han, X. Liu, X. Wei, and X. Zhu, "Reduced-order observer-based finite time fault estimation for switched systems with lager and fast time varying fault," *IEEE Trans. Circuits Syst. II, Exp. Briefs*, vol. 71, no. 1, pp. 350–354, Jan. 2024, doi: [10.1109/TCSII.2023.3304271](https://doi.org/10.1109/TCSII.2023.3304271).
- [37] J. Han, X. Liu, X. Xie, and X. Wei, "Dynamic output feedback fault tolerant control for switched fuzzy systems with fast time varying and unbounded faults," *IEEE Trans. Fuzzy Syst.*, vol. 31, no. 9, pp. 3185–3196, Feb. 2023, doi: [10.1109/TFUZZ.2023.3246061](https://doi.org/10.1109/TFUZZ.2023.3246061).
- [38] N. K. Nichols and D. Chu, "Regularization of descriptor systems," in *Numerical Algebra, Matrix Theory, Differential-Algebraic Equations and Control Theory*, 1st ed, Cham, Switzerland: Springer, 2015, pp. 415–433. [Online]. Available: <http://www.link.springer.com>
- [39] W. L. Luyben, *Practical Distillation Control*. New York, NY, USA: Springer, 1992.
- [40] S. Skogestad, "Dynamics and control of distillation columns," *Chem. Eng. Res. Des.*, vol. 75, no. 6, pp. 539–562, Sep. 1997, doi: [10.1205/026387697524092](https://doi.org/10.1205/026387697524092).
- [41] D. W. Green and R. H. Perry, *Perry's Chemical Engineer's Handbook*. New York, NY, USA: McGraw-Hill, 2007.
- [42] H. Hamdi, M. Rodrigues, C. Mechmeche, D. Theilliol, and N. B. Braiek, "Fault detection and isolation in linear parameter-varying descriptor systems via proportional integral observer," *Int. J. Adapt. Control Signal Process.*, vol. 26, no. 3, pp. 224–240, Mar. 2012, doi: [10.1002/acs.1260](https://doi.org/10.1002/acs.1260).
- [43] A. Aguilera-González, D. Theilliol, M. Adam-Medina, C. M. Astorga-Zaragoza, and M. Rodrigues, "Sensor fault and unknown input estimation based on proportional integral observer applied to LPV descriptor systems," *IFAC Proc. Volumes*, vol. 45, no. 20, pp. 1059–1064, Jan. 2012, doi: [10.3182/20120829-3-mx-2028.00177](https://doi.org/10.3182/20120829-3-mx-2028.00177).
- [44] J. Lofberg, "YALMIP: A toolbox for modeling and optimization in MATLAB," in *Proc. IEEE Int. Conf. Robot. Autom.*, Taiwan, Sep. 2004, pp. 284–289, doi: [10.1109/CACSD.2004.1393890](https://doi.org/10.1109/CACSD.2004.1393890).
- [45] C. Edwards and C. P. Tan, "A comparison of sliding mode and unknown input observers for fault reconstruction," *Eur. J. Control*, vol. 12, no. 3, pp. 245–260, Jan. 2006.
- [46] G. R. Duan, *Analysis and Design of Descriptor Linear Systems*. Berlin, Germany: Springer, 2010.



CARLOS MANUEL ASTORGA-ZARAGOZA received the Ph.D. degree in process engineering from Université Claude Bernard Lyon 1, France, in 2001. Since 1993, he has held teaching and research positions with the Tecnológico Nacional de México/CENIDET. His research interests include observers and fault detection systems for energy conversion processes.



GLORIA LILIA OSORIO-GORDILLO received the M.Sc. degree from the Centro Nacional de Investigación y Desarrollo Tecnológico (CENIDET), Mexico, in 2011, and the double Ph.D. degree in automatic control from the University of Lorraine, France, and TECNM/CENIDET, in 2015. She has been a Research Professor with CENIDET, since 2015. Her research interests include observers design for descriptor, singular, Takagi–Sugeno, LPV systems, fault diagnosis, and fault tolerant control.



RODOLFO AMALIO VARGAS-MÉNDEZ received the M.Sc. degree in electronic engineering and the Ph.D. degree in electronics engineering in the area of power electronics from the Centro Nacional de Investigación y Desarrollo Tecnológico (CENIDET), Mexico, in 2011 and 2015, respectively. He has been a Research Professor with CENIDET, since 2016. His research interests include multilevel inverters symmetric and asymmetric topologies, carrier-based PWM methods, space-vector modulation, and fault-tolerant systems.



PORFIRIO-ROBERTO NÁJERA-MEDINA received the B.S. degree in communications and electronics engineering from the Instituto Politécnico Nacional, Mexico, and the M.Sc. degree in electronic engineering from the Centro Nacional de Investigación y Desarrollo Tecnológico (CENIDET), Cuernavaca, Mexico. He is currently a full-time Professor and a Researcher with the Electrical and Electronic Engineering Department, Instituto Tecnológico de Cuautla, Yecapixtla, Mexico. He has participated in diverse innovation and creativity projects, obtaining several first places nationwide. His research interests include power electronics, energy management, renewable energy, and energy conversion.



has participated in diverse projects funded by the Tecnológico Nacional de México. Her research interests include fault diagnosis, fault tolerant control, process control, dynamic systems modeling, machine learning, and robotics.

MARLEM FLORES-MONTIEL (Member, IEEE) received the B.S. degree in electronic engineering from the Instituto Tecnológico de Cuautla, Mexico, in 2010, and the M.Sc. degree in electronic engineering from the Centro Nacional de Investigación y Desarrollo Tecnológico (CENIDET), Cuernavaca, Mexico, in 2012. She is currently a Professor with the Electrical and Electronic Engineering Department, Instituto Tecnológico de Cuautla, Yecapixtla, Mexico.



ANGÉLICA GÓMEZ-CÁRDENAS received the B.S. degree in certified public accountant from Universidad Autónoma del Estado de Morelos, Mexico, in 1996, and the M.B.A. degree from the Instituto Tecnológico de Zacatepec, Mexico, in 2006. She is currently a Professor and a Researcher with the Economic Administrative Sciences Department, Instituto Tecnológico de Cuautla, Yecapixtla, Mexico. Her research interests include leadership institutional management and technology in educational administration.